Data Repository item 2005098

Data Repository
Evolution of a volcanic rifted margin: southern Red Sea, Ethiopia

Results from $^{40}Ar/^{39}Ar$ isotope analyses.

E. Wolfenden, C. J. Ebinger, Gezahegn Yirgu, P. R. Renne & S. P. Kelley

Analytical Methods

Samples of volcanic rocks were prepared Royal Holloway University of London for $^{40}Ar/^{39}Ar$ analyses. Analyses of samples EEW00-1, EEW00-17 and EEW00-21 were carried out at Berkeley Geochronology Center, as per Ukstins *et al.* (2002). Fish Canyon sanidine (FCs) was used as a neutron flux monitor at Oregon State University. The calculated mean J-value, which reflects total variation in neutron flux during irradiation, was 0.0013221 ± 0.0000432. Sample analysis was by multi-crystal step heating of both plagioclase and groundmass for EEW00-1 and EEW00-17, to constrain variations in accuracy of ages for different phases, and a mixture of plagioclase and alkali-feldspars for EEW00-21 (Table 1).

Analyses of samples EEW02-2, EEW02-5, EEW02-20, EEW99M2 and EEW00-30 were carried out at the Geology Department, The Open University, with irradiation of samples at McMaster University. GA15 50 biotite was used as a neutron flux monitor, and calibrated against Fish Canyon sanidine (FCs, 28.02 Ma) following Renne (1998). The calculated mean J-value was 0.01203 ± 0.00006. Samples were analysed in 1 batch on a MAP 215-50 mass spectrometer (plus a re-analysis of EEW00-7), heating by laser with a Nd-YAG. Sample analysis was by multi-crystal step heating with a CO_2 laser and integrator lens of 30-100 grains of groundmass of EEW02-2, and EEW02-20, and alkali feldspar for EEW00-30, EEW99M2 and EEW020-5 (Table 2). Argon isotopic analyses were made with an MAP 215-50 mass spectrometer. Procedural blanks and nuclear interference corrections were as reported by Knight et al. (2003). Mass discrimination (1.0062 ± 0.0013 per amu) was monitored by automated analysis of 55 air pipettes interspersed with the samples, and correction was made based on a power-law relationship.

Accuracy of analyses was monitored with procedural blanks, which contained < 1% of measured ^{40}Ar. CaF_2 and K_2SO_4 were analysed between samples for periodic calibration. Background levels of ^{35}Cl and $^{41}CxHy$ contamination were also monitored.

Data Analysis

Plateau ages and integrated ages for samples analysed at Berkeley Geochronology Center are listed in Table DR1 and the steps used to define plateaus are shown in Figures DR2-DR6. Plateau ages for samples analysed at the Open University are listed in Table DR2 and the steps used to define plateaus, as per Ludwig (2003), are shown in Figures DR7 –DR8. Plateaux for both labs were defined as comprising at least 3 consecutive steps containing at least 50% of the ^{39}Ar released. Note that the release in sample EEW30 is dominated by two steps (Fig DR8b). The weighted mean of all steps is 26.00 ± 0.34 Ma, and the total fusion age is 26.1±0.3 Ma, indicating that the age is robust.

Stratigraphy

Below we provide additional observations used to delineate stratigraphic packages and to interpret the evolution of the southern Red Sea margin in Afar.

Volcano-stratigraphy: A-A'

The volcanic packages observed at 11°N to 11°15'N and between 39°30'E and 40°E are laterally homogeneous if not continuous for 10's of km, and comprise dominantly basaltic lava flows with minor intercalated ignimbrites, air-fall tuffs and rhyolites. This flood volcanic stratigraphy is similar to that described by Zanettin and Justin-Visentin (1975) and to that dated at 31-28 Ma by Hofmann *et al.*, (1997). Flood volcanic sequences described by Hofmann *et al.* (1997) at localities 50 km further to the north and west of section A-A' are up to 2000 m thick, the thickness assumed here. An age of 29.43 ± 0.12 Ma was obtained for an ignimbrite east of the Borkena graben confirming that it lies towards the top of the flood volcanic group (Ukstins *et al.* 2002). West of the Borkena graben two ignimbrites at 2760 m and

2780 m near the top of the flood volcanic group were dated at 30.16 Ma ± 0.12 Ma and 29.61 ± 0.12 Ma (Ukstins *et al.* 2002) (Fig. 4).

Contacts of flood volcanic units with overlying basalt flows are exposed immediately to the west and east of the fault bounded Borkena graben (Fig. 5). The overlying basalt centres and flows are morphologically distinct from the flood volcanic successions (Table DR3). We the term the overlying basaltic package the *Dese basalt formation* (Table DR3). Plagioclase separates from two basaltic flows within this package were dated at 25.1 ± 0.2 Ma and 25.0 ± 0.2 Ma (Ukstins *et al.*, 2002). Flows around constructs dip more steeply than the flood basalts with the "excess" dip of the upper units caused by flow morphology and volcanic construction rather than rotation on fault blocks.

At the eastern end of section A-A' the "younger volcanics" of Morton and Black (1975) and "Quaternary basalts" of Chorowicz *et al.* (1999), are divided into two distinct packages: intercalated basalts and rhyolites named the *Burka formation* (this study) and fissural basalts, the Dahla Series (J. Quade pers. comm., 2002)(Fig. 4). The *Burka formation* is as yet undated but it offlaps flood basaltic units east of 40°E, dated 30.92 ± 0.11 Ma (Ukstins et al. 2002). The flood basalt flows adjacent to the Burka formation are dyked but dykes are exclusively mafic suggesting that emplacement of silicic units was restricted to the east. The *Burka formation* is offlapped by the Dahla Series. The Dahla Series is separated from underlying formations by a regionally extensive tectonic unconformity that, where dated, is ~6 My (see below). The Dahla Series was previously inferred to be older than the hominid-bearing 5.3 Ma Sagantole Formation (J. Quade, pers. comm., 2002).

Volcano-stratigraphy: B-B' and C-C'

A composite volcano-stratigraphy for cross-sections B-B' and C-C' is shown in Figure 4. In section B-B' flood basalts are down-thrown to the east and juxtaposed against rhyolitic centers and near-source flows and breccias (Fig. 5). In section C-C', unlike section A-A', the flood volcanic group is not exposed east of the Borkena Graben but is presumably buried beneath a minimum of 1500 m of rhyolites (DR3). This rhyolitic complex is informally named the *Kemise rhyolite formation* (this study), and forms both west and east sides of the Borkena Graben between 10°15'N and 11°N. A rhyolitic lava, EEW00-30, from west of the Borkena Graben was dated at 25.90 ± 0.16 Ma (Table 2).

Massive fissural basalts intruded by rhyolite domes occur in exposures east of 40°E. We term this sequence the *Aneno formation,* which has flows extensive over 4 km but no visible intrusive centers suggesting that the lavas were fed by dikes. The *Aneno formation* thickens rapidly eastwards to at least 200 m. A basalt lava, EEW00-2, at the base of a 300 m exposed section, including overlying formations, was dated at 15.9 ± 0.5 Ma (Table 1).

East of the *Kemise rhyolitic formation*, across a faulted contact, are at least 400 m of basaltic to intermediate centers marked by eroded basaltic cones and associated lava flows a few metres thick, scoriaceous basaltic flows and intermediate lava flows. One of the top-most of the intermediate lavas, EEW00-21, was dated at 7.12 ± 0.04 Ma (Table 2). These basaltic to intermediate lavas are named the *Bercha formation.*

East of 40°E the *Aneno formation,* and where present the Bercha formation, is unconformably overlain by *ca.* 60 m of discontinuous, feldspar-rich fluvial sediments and flat-lying outliers of the fissural basaltic Dahla Series. A basalt flow forming the

western edge of the Dahla Series was dated at 6.64 ± 0.04 Ma (Table 2). The Dahla Series thickens from less than 50 m at the dated unit to around 200 m just 4 km to the east.

Volcano-stratigraphy: D-D'

Cross-section D-D' lies *ca.* 20 km south of section B-B' (Figs. 2,5). The overall stratigraphy follows a similar pattern to C-C' and B-B'(Figs. 4, 7, 9). At ~3200 m elevation the flood volcanic group is disconformably overlain by about 100 m of massive rhyolitic flows, e.g. EEWM2 dated at 26.47± 0.15 Ma (Table 2) (Fig. 10). These rhyolites are informally named the *Ataye rhyolite formation* here.

There are disconformities between the top-most flood volcanic units and the *Ataye rhyolite formation*, and between the *Ataye rhyolite formation* and overlying basaltic shield volcanoes. A rhyolitic ignimbrite of the *Ataye rhyolite formation* occurring immediately east of a marginal graben was dated at 25.30 Ma ± 0.13 Ma (Ukstins *et al.,* 2002).

Overlying the *Ataye rhyolite formation* and west of the marginal graben are up to 200 m of thin dominantly basaltic units named the *Sar Amba formation* (Table DR3). Overlying the *Sar Amba formation* are 300 m of ignimbrites and rhyolitic ignimbrites, named the *Gadilo ignimbrite formation.* The *Sar Amba* and *Gadilo ignimbrite formations* are laterally extensive and drape the *Ataye rhyolite formation* (Fig. 10).

East and west of the marginal graben, intruding the *Ataye rhyolite, Sar Amba* and *Gadilo ignimbrite formations* adjacent to normal fault planes is the *Kile rhyolite formation* (Table DR3). Also overlying the *Gadilo ignimbrite formation* is a second dominantly basaltic package the *Mehal Wenz formation* (DC3).

Overlying all the earlier stratigraphy in this section is the *Senbete ignimbrite formation.* It comprises ignimbrite-tuff pairs from an unknown but more distal source than the centers feeding the *Ataye* or *Kile rhyolite formations.* There are laterally extensive unconformities between the *Ataye rhyolitic formation* and the basaltic *Sar Amba formation* and between the *Gadilo ignimbritic formation* and the *Mehal Wenz formation.* There is also an extensive unconformity between the *Senbete ignimbrite formation* and the *Kile rhyolite formation.* The lowermost ignimbrite unit of the *Senbete ignimbrite formation,* sample EEW02-5, was dated at 24.80 ± 0.13 Ma (Table 2).

Volcano-stratigraphy: E-E'

The flood volcanic group is 1000 m thick ~ 50 km west of profile E-E', which is the thickness inferred for E-E' (Fig. 11), and it overlies Archean-Proterozoic basement and Jurassic marine sediments (R. Pik, pers. comm., 2003). The flood volcanic group is juxtaposed against rhyolitic centers that are overlain by basaltic centers, including EEW00-1, which is a 24.59 ± 0.16 Ma basaltic flow at the base of the basaltic pile (Figs. 5, 11, Table 1). These Lower Miocene basaltic centers and associated lavas are named the *Birkitu formation.* Overlying these basalts are dominantly ignimbritic units with minor intercalated basaltic products of the *Shewa Robit ignimbrite formation.* This formation spans an age range of at least 19.76 ± 0.07 Ma to 14.90 ± 0.06 Ma (Ukstins *et al.*, 2002). Capping the stratigraphy on the plateau are trachytic shield volcanoes inferred to be Mid-Miocene by Mohr (1983), and named the Termaber Formation (Fig. 4). Two of these complexes, Megezez and Mezezo, have been dated at 10.87± 0.06 Ma (Ukstins *et al.*, 2002) and 10.5 ± 0.2 Ma (George, 1997), respectively.

Similar to sections further north a marginal graben covered with alluvium is present between the uplifted Lower Miocene *Birkitu basalt formation*, and the Lower-Mid Miocene *Shewa Robit ignimbrite formation.* East of and co-incident with the faults defining the eastern side of the marginal graben is a second complex of rhyolitic centers at least 400 m thick, these are named the *Insertu formation.* The *Insertu formation* overlies the Lower Miocene *Birkitu basalt formation.* The *Insertu formation* intrudes and is overlain by further ignimbrite and tuff units of the *Shewa Robit formation* (Fig. 10).

Volcano-stratigraphy: F-F'

The western side of Profile F-F' crosses the top of the flood volcanic group, which remains undated at this locality (Figs. 4, 5,11). Ignimbrites overlying flood basalts on the plateau were dated at 11.59 ± 0.06 Ma, and at 11.73 ± 0.05 Ma and 11.70 ± 0.04 Ma in the Baso-Werena basin (Ukstins *et al.*, 2002). The ignimbrites are much thicker within the rift basin (800 m) than on the plateau (< 50 m) where they drape the flood volcanic group. This synrift ignimbrite formation is named the *Aliyu Amba ignimbrite formation.* The similar ages of ignimbrite flows from the *Aliyu Amba formation* in the rift basin and on the plateau suggests that little stratigraphy has been removed from the plateau above the flood basalts and that thickness variations seen today are representative of those originally emplaced. The ignimbrites in the rift basin are intruded by smaller volume rhyolites in <100 m-wide fault zones.

Unconformably overlying the *Aliyu Amba ignimbrite formation* are around 500 m of basaltic centers and contemporaneous dike-fed basaltic flows. These are named the *Astit formation.* Overlying or interdigitating with the *Astit formation* is the 500 m-thick trachytic shield complex of Mezezo; one of the top-most flows is dated at 10.87 ± 0.06 Ma (Ukstins *et al.*, 2002). At the eastern end of section F-F' are several

trachytic flows. A flow from the base of the >200 m-thick sequence, EEW02-20, was dated at 3.50 ± 0.11 Ma (Table 2). This sequence offlaps units below and to the west.

References

Ludwig, K., 2003, ISOPLOT a geochronological tool kit for Microsoft excel, Berkeley Geochronology Centre Special Publication, No. 4, 71 pp.

Knight, K., Renne, P. R., Halkett, A., and White, N., 2003, 40Ar/39Ar dating of the Rajahmundry Traps, eastern India, and their relationship to the Deccan traps, Earth and Planetary Science Letters, v. 208, p. 85-99.

Renne, P.R., Swisher, C.S., Deino, A.L., Karner, D.B., Owens, D.J., and DePaolo, D.J., 1998, Intercalibration of standards, absolute ages and uncertainties in $^{40}Ar/^{39}Ar$ dating, Chemical Geology, v. 145, p. 117-152.

Ukstins I.A., Renne, P.R., Wolfenden, E., Baker, J., Ayalew, D., and Menzies, M., 2002, Matching conjugate volcanic rifted margins: $^{40}Ar/^{39}Ar$ chrono-stratigraphy of pre- and syn-rift bimodal flood volcanism in Ethiopia and Yemen, Earth And Planetary Science Letters, v. 198, p. 289-306.

Wolfenden E., 2003, Evolution of the southern Red Sea Rift: Birth of a magmatic margin, Phd thesis (unpublished), Royal Holloway University of London, 298 pp.

Table DR1

Laser Power (W)	^{40}Ar (moles)	^{40}Ar (nAmps)	± σ (nAmps)	^{39}Ar (nAmps)	± σ (nAmps)	^{38}Ar (nAmps)	± σ (nAmps)	^{37}Ar (nAmps)	± σ (nAmps)	^{36}Ar (nAmps)	± σ (nAmps)	$^{40}Ar^*/^{39}Ar_K$	± σ	$\%^{40}Ar^*$	Age (Ma)	± Age (Ma)
EEW1 whole rock	J = 0.0013221 ± 4.32e-6															
1	8.55E-15	0.82195	0.00169	0.00613	0.00010	0.00045	0.00002	0.00414	0.00006	0.00216	0.00003	30.00837	1.51092	22.4	70.19	3.47
1.5	2.27E-14	2.18443	0.00294	0.02035	0.00012	0.00129	0.00002	0.01512	0.00009	0.00544	0.00004	28.36272	0.73527	26.4	66.41	1.69
2	1.90E-14	1.82528	0.00210	0.02963	0.00014	0.00116	0.00002	0.02563	0.00013	0.00405	0.00003	21.31920	0.42083	34.6	50.15	0.98
2.5	1.49E-14	1.43651	0.00196	0.05233	0.00017	0.00110	0.00002	0.05064	0.00016	0.00238	0.00003	14.12365	0.18731	51.4	33.38	0.44
3	1.61E-14	1.55201	0.00189	0.09925	0.00024	0.00147	0.00002	0.09298	0.00022	0.00122	0.00002	12.08466	0.08715	77.2	28.60	0.20
3.5	1.98E-14	1.90568	0.00203	0.15474	0.00027	0.00189	0.00002	0.13600	0.00033	0.00050	0.00002	11.43409	0.04993	92.8	27.07	0.12
4	2.39E-14	2.30392	0.00294	0.20312	0.00031	0.00248	0.00002	0.16958	0.00050	0.00030	0.00002	10.97558	0.04142	96.7	25.99	0.10
4.5	2.94E-14	2.82691	0.00303	0.25523	0.00052	0.00304	0.00003	0.20633	0.00061	0.00021	0.00002	10.90541	0.03794	98.4	25.83	0.09
5	3.70E-14	3.56468	0.00394	0.32965	0.00068	0.00394	0.00003	0.25162	0.00052	0.00020	0.00002	10.70249	0.03547	98.9	25.35	0.08
5.5	3.41E-14	3.28625	0.00276	0.30695	0.00045	0.00365	0.00003	0.22577	0.00065	0.00017	0.00002	10.60939	0.02999	99.0	25.13	0.07
6	3.33E-14	3.20411	0.00294	0.30270	0.00057	0.00359	0.00003	0.21976	0.00070	0.00013	0.00002	10.51886	0.03291	99.3	24.92	0.08
6.5	2.91E-14	2.79752	0.00294	0.26455	0.00054	0.00323	0.00003	0.19431	0.00057	0.00012	0.00002	10.49826	0.03653	99.2	24.87	0.09
7	2.23E-14	2.14460	0.00226	0.20467	0.00035	0.00249	0.00003	0.15985	0.00031	0.00012	0.00002	10.36634	0.03753	98.9	24.56	0.09
7.5	1.63E-14	1.56793	0.00203	0.14892	0.00028	0.00182	0.00002	0.12228	0.00024	0.00008	0.00002	10.44485	0.04620	99.1	24.74	0.11
8	1.35E-14	1.30250	0.00196	0.12414	0.00025	0.00158	0.00003	0.10837	0.00027	0.00011	0.00002	10.30298	0.05339	98.1	24.41	0.13
9	1.36E-14	1.31005	0.00167	0.12470	0.00021	0.00155	0.00002	0.12151	0.00024	0.00013	0.00002	10.28236	0.05134	97.8	24.36	0.12
10	1.18E-14	1.13994	0.00168	0.10696	0.00024	0.00137	0.00002	0.12429	0.00024	0.00020	0.00002	10.19829	0.06192	95.6	24.16	0.15
11	7.31E-15	0.70332	0.00175	0.06522	0.00021	0.00085	0.00002	0.08939	0.00021	0.00017	0.00002	10.14758	0.09821	94.0	24.04	0.23
12	6.89E-15	0.66312	0.00158	0.06048	0.00017	0.00083	0.00002	0.23209	0.00072	0.00026	0.00002	10.01970	0.10640	91.1	23.74	0.25
14	4.76E-15	0.45758	0.00146	0.04049	0.00017	0.00061	0.00002	0.35960	0.00081	0.00030	0.00002	9.90084	0.16235	87.0	23.46	0.38
16	2.34E-15	0.22504	0.00147	0.01891	0.00012	0.00029	0.00002	0.21455	0.00064	0.00019	0.00002	9.82669	0.31967	81.9	23.29	0.75
18	1.24E-15	0.11805	0.00142	0.00927	0.00010	0.00016	0.00002	0.10505	0.00031	0.00013	0.00002	9.48896	0.60211	73.9	22.49	1.42
21	9.99E-16	0.09514	0.00140	0.00684	0.00010	0.00012	0.00002	0.09571	0.00031	0.00014	0.00002	9.18114	0.84498	65.3	21.77	1.99
25	1.01E-15	0.09599	0.00140	0.00655	0.00010	0.00010	0.00002	0.10318	0.00031	0.00011	0.00002	11.23438	0.86393	75.7	26.60	2.03
EEW-17 whole rock	J = 0.0013221 ± 4.32e-6															
1	5.49E-15	0.52694	0.00161	0.00561	0.00010	0.00042	0.00002	0.01944	0.00011	0.00173	0.00003	2.82297	1.55026	3.0	6.72	3.68
1.5	1.06E-14	1.01897	0.00182	0.01292	0.00012	0.00080	0.00002	0.06789	0.00018	0.00334	0.00003	2.87273	0.84245	3.6	6.84	2.00
2	1.49E-14	1.43209	0.00203	0.02233	0.00014	0.00118	0.00002	0.07304	0.00021	0.00469	0.00004	2.37268	0.59630	3.7	5.65	1.42
2.5	1.09E-14	1.05188	0.00175	0.03584	0.00010	0.00107	0.00002	0.09922	0.00025	0.00320	0.00003	3.16646	0.29479	10.8	7.54	0.70
3	7.93E-15	0.76276	0.00175	0.05997	0.00019	0.00107	0.00002	0.13730	0.00040	0.00201	0.00003	2.97647	0.15280	23.4	7.09	0.36
3.5	8.53E-15	0.82099	0.00169	0.08763	0.00029	0.00141	0.00003	0.17656	0.00047	0.00194	0.00003	3.00143	0.10727	32.0	7.14	0.25
4	9.80E-15	0.94319	0.00195	0.11333	0.00029	0.00171	0.00002	0.20321	0.00064	0.00215	0.00003	2.85183	0.08267	34.2	6.79	0.20
4.5	1.03E-14	0.98776	0.00175	0.15965	0.00019	0.00219	0.00003	0.27014	0.00062	0.00188	0.00002	2.84652	0.04201	46.0	6.78	0.10
5	8.66E-15	0.83315	0.00182	0.19282	0.00034	0.00259	0.00003	0.28493	0.00064	0.00104	0.00002	2.84800	0.04142	65.8	6.78	0.10
5.5	8.46E-15	0.81360	0.00169	0.20830	0.00036	0.00264	0.00003	0.27328	0.00082	0.00087	0.00002	2.78219	0.03688	71.2	6.62	0.09
6	8.04E-15	0.77245	0.00167	0.19240	0.00032	0.00248	0.00003	0.22242	0.00058	0.00087	0.00002	2.76622	0.03863	68.9	6.59	0.09
6.5	8.06E-15	0.77443	0.00165	0.17323	0.00028	0.00228	0.00003	0.17939	0.00040	0.00104	0.00002	2.77150	0.04433	62.0	6.60	0.11
7	8.32E-15	0.80015	0.00175	0.16722	0.00031	0.00220	0.00003	0.15779	0.00029	0.00118	0.00002	2.76609	0.04644	57.8	6.59	0.11
7.5	7.48E-15	0.72014	0.00175	0.14820	0.00029	0.00203	0.00003	0.13192	0.00036	0.00109	0.00002	2.75126	0.05194	56.6	6.55	0.12
8	7.89E-15	0.75910	0.00162	0.15827	0.00029	0.00216	0.00003	0.13861	0.00040	0.00109	0.00002	2.82945	0.04993	59.0	6.74	0.12
9	8.35E-15	0.80274	0.00166	0.17140	0.00025	0.00236	0.00003	0.17371	0.00042	0.00117	0.00002	2.75263	0.04261	58.7	6.55	0.10
10	7.59E-15	0.73317	0.00150	0.17159	0.00017	0.00234	0.00003	0.23524	0.00107	0.00096	0.00002	2.73518	0.04419	64.0	6.51	0.11
11	3.55E-15	0.34197	0.00158	0.08294	0.00012	0.00107	0.00002	0.14724	0.00034	0.00042	0.00002	2.75085	0.06297	66.6	6.55	0.15
12	2.29E-15	0.21861	0.00148	0.05564	0.00018	0.00072	0.00002	0.10134	0.00032	0.00024	0.00002	2.80335	0.10260	71.3	6.67	0.24
14	2.53E-15	0.24440	0.00143	0.05829	0.00012	0.00077	0.00002	0.14437	0.00027	0.00032	0.00002	2.78600	0.08676	66.3	6.63	0.21
16	2.37E-15	0.22672	0.00158	0.05485	0.00020	0.00074	0.00002	0.16778	0.00043	0.00028	0.00002	2.87388	0.10501	69.4	6.84	0.25
18	2.16E-15	0.20731	0.00147	0.04994	0.00017	0.00069	0.00002	0.17893	0.00038	0.00024	0.00002	3.01936	0.11803	72.5	7.19	0.28
21	2.52E-15	0.25004	0.00145	0.05368	0.00015	0.00075	0.00002	0.22806	0.00058	0.00031	0.00002	3.30562	0.09354	70.8	7.87	0.22
25	2.53E-15	0.24692	0.00144	0.04696	0.00012	0.00064	0.00002	0.19778	0.00049	0.00026	0.00002	3.96578	0.10674	75.2	9.43	0.25
EEW1 plag	J = 0.0013221 ± 4.32e-6															
1	3.05E-15	0.29587	0.00148	0.00146	0.00008	0.00018	0.00002	0.01000	0.00008	0.00093	0.00002	15.57628	4.89332	7.6	36.77	11.44
2	1.32E-15	0.12929	0.00142	0.00436	0.00008	0.00009	0.00002	0.04861	0.00021	0.00026	0.00002	12.87918	1.37303	43.0	30.46	3.22
3	1.82E-15	0.17735	0.00143	0.01073	0.00009	0.00018	0.00002	0.13141	0.00036	0.00024	0.00002	11.03512	0.54101	66.2	26.13	1.27
4	2.24E-15	0.21441	0.00143	0.01542	0.00010	0.00024	0.00002	0.19678	0.00044	0.00026	0.00002	10.07616	0.32825	71.8	23.87	0.77
5	2.99E-15	0.28681	0.00144	0.02397	0.00011	0.00031	0.00002	0.31486	0.00069	0.00020	0.00002	10.66549	0.25307	88.2	25.26	0.60
6	3.47E-15	0.33345	0.00158	0.02950	0.00012	0.00039	0.00002	0.38417	0.00058	0.00021	0.00002	10.29442	0.20813	90.2	24.39	0.49
7	4.17E-15	0.40045	0.00156	0.03507	0.00014	0.00044	0.00002	0.46331	0.00099	0.00023	0.00002	10.59772	0.18259	91.9	25.10	0.43
8	4.79E-15	0.45988	0.00157	0.04096	0.00015	0.00053	0.00002	0.53072	0.00148	0.00030	0.00002	10.20562	0.15759	90.0	24.18	0.37
10	7.19E-15	0.69066	0.00169	0.06030	0.00017	0.00078	0.00002	0.78358	0.00201	0.00043	0.00002	10.46394	0.11777	90.5	24.79	0.28
12	4.31E-15	0.41584	0.00145	0.03729	0.00013	0.00046	0.00002	0.48172	0.00113	0.00026	0.00002	10.17841	0.16557	90.4	24.12	0.39
14	3.33E-15	0.31939	0.00143	0.02925	0.00012	0.00036	0.00002	0.38294	0.00129	0.00015	0.00002	10.48787	0.20850	95.1	24.84	0.49
16	2.54E-15	0.24325	0.00148	0.02195	0.00012	0.00029	0.00002	0.28638	0.00097	0.00013	0.00002	10.41299	0.26834	93.0	24.67	0.63
18	2.02E-15	0.19348	0.00147	0.01730	0.00012	0.00019	0.00001	0.22932	0.00069	0.00011	0.00002	10.43253	0.33959	92.4	24.71	0.80
21	1.93E-15	0.18414	0.00144	0.01701	0.00009	0.00023	0.00002	0.21828	0.00064	0.00009	0.00002	10.37952	0.34182	94.9	24.59	0.80
25	1.69E-15	0.16156	0.00142	0.01456	0.00008	0.00019	0.00002	0.18677	0.00053	0.00011	0.00002	9.88059	0.38532	88.2	23.41	0.91
EEW17 plag	J = 0.0013221 ± 4.32e-6															
1	2.03E-16	0.01846	0.00137	0.00069	0.00007	0.00002	0.00001	0.00162	0.00007	0.00005	0.00002	6.59825	6.96634	24.6	15.67	16.47
2	1.29E-15	0.11974	0.00143	0.00366	0.00007	0.00007	0.00002	0.00694	0.00015	0.00025	0.00002	12.62285	1.36636	38.6	29.86	3.21
3	1.67E-15	0.15486	0.00139	0.00235	0.00007	0.00011	0.00001	0.00655	0.00015	0.00044	0.00002	11.12649	2.14988	16.9	26.35	5.05
4	1.82E-15	0.16988	0.00139	0.00251	0.00007	0.00015	0.00002	0.00859	0.00010	0.00052	0.00002	6.38586	2.02197	9.4	15.17	4.78
5	1.60E-15	0.14797	0.00139	0.00194	0.00007	0.00009	0.00001	0.01361	0.00016	0.00046	0.00002	6.30722	2.59232	8.2	14.98	6.13
6	1.89E-15	0.17594	0.00146	0.00528	0.00008	0.00012	0.00001	0.03395	0.00024	0.00055	0.00002	3.05216	0.97128	9.1	7.27	2.31
7	2.05E-15	0.18997	0.00146	0.00842	0.00008	0.00021	0.00002	0.05165	0.00037	0.00057	0.00002	3.15499	0.60969	13.9	7.51	1.45
8	1.50E-15	0.13850	0.00163	0.01108	0.00009	0.00019	0.00002	0.05600	0.00034	0.00034	0.00002	3.76879	0.53533	30.0	8.97	1.27
10	6.19E-16	0.05744	0.00141	0.00759	0.00008	0.00012	0.00001	0.05723	0.00031	0.00011	0.00002	4.02142	0.72701	52.8	9.57	1.72
12	2.61E-16	0.02333	0.00139	0.00548	0.00008	0.00007	0.00001	0.05141	0.00031	0.00003	0.00002	3.26599	0.87688	76.2	7.77	2.08
14	2.81E-16	0.02507	0.00139	0.00584	0.00008	0.00006	0.00001	0.05430	0.00034	0.00004	0.00002	2.94578	0.89992	68.1	7.01	2.14
16	9.32E-17	0.00811	0.00137	0.00207	0.00007	0.00004	0.00001	0.01770	0.00019	0.00001	0.00002	2.66650	2.52322	67.5	6.35	6.00
18	2.62E-17	0.00203	0.00137	0.00080	0.00007	-0.00001	0.00001	0.00518	0.00011	0.00000	0.00002	2.18744	5.96564	85.8	5.21	14.19
21	1.60E-16	0.01493	0.00137	0.00313	0.00008	0.00003	0.00001	0.02955	0.00016	0.00002	0.00002	3.21411	1.66950	66.9	7.65	3.97
25	1.81E-16	0.01627	0.00139	0.00481	0.00008	0.00006	0.00001	0.04586	0.00020	0.00001	0.00002	3.32894	1.07964	97.7	7.92	2.56
EEW21 plag	J = 0.0013221 ± 4.32e-6															
1	2.07E-15	0.19798	0.00147	0.00284	0.00008	0.00016	0.00002	0.01041	0.00011	0.00066	0.00002	1.09661	2.22183	1.6	2.61	5.29
2	2.19E-15	0.20984	0.00153	0.02790	0.00013	0.00041	0.00002	0.11486	0.00034	0.00048	0.00002	2.81762	0.21917	37.4	6.71	0.52
3	2.33E-15	0.22365	0.00150	0.05856	0.00016	0.00073	0.00002	0.24178	0.00073	0.00025	0.00002	2.87230	0.10420	75.0	6.84	0.25
4	2.68E-15	0.25687	0.00141	0.07621	0.00016	0.00090	0.00002	0.27391	0.00104	0.00014	0.00002	3.10566	0.07737	91.9	7.39	0.18
5	3.31E-15	0.31913	0.00145	0.09690	0.00012	0.00120	0.00002	0.30411	0.00163	0.00019	0.00002	2.95746	0.06293	89.6	7.04	0.15
6	4.59E-15	0.44075	0.00162	0.13662	0.00021	0.00165	0.00003	0.33159	0.00070	0.00020	0.00002	2.99467	0.04526	92.7	7.13	0.11
7	6.63E-15	0.63789	0.00168	0.19927	0.00024	0.00245	0.00003	0.35077	0.00101	0.00025	0.00002	2.97803	0.03138	92.9	7.09	0.07
8	8.74E-15	0.84024	0.00175	0.25755	0.00046	0.00310	0.00003	0.30298	0.00085	0.00035	0.00002	2.95739	0.02646	90.6	7.04	0.06
10	1.21E-14	1.16655	0.00182	0.31298	0.00050	0.00389	0.00003	0.43242	0.00087	0.00089	0.00002	3.00063	0.02351	80.4	7.14	0.06
12	6.44E-15	0.61956	0.00163	0.17728	0.00024	0.00225	0.00002	0.27355	0.00071	0.00037	0.00002	3.00301	0.03524	85.8	7.15	0.08
14	5.22E-15	0.50234	0.00159	0.14341	0.00025	0.00184	0.00002	0.21567	0.00048	0.00030	0.00002	3.01256	0.04319	85.9	7.17	0.10
16	2.44E-15	0.23396	0.00147	0.06547	0.00018	0.00081	0.00002	0.16236	0.00034	0.00018	0.00002	2.96771	0.09008	82.9	7.06	0.21
18	1.84E-15	0.17694	0.00141	0.04485	0.00014	0.00057	0.00002	0.14192	0.00037	0.00017	0.00002	3.08667	0.13085	78.1	7.35	0.31
21	1.77E-15	0.16952	0.00138	0.04344	0.00011	0.00057	0.00002	0.14511	0.00034	0.00017	0.00002	2.99409	0.11263	76.5	7.13	0.27
25	2.27E-15	0.21847	0.00147	0.05744	0.00016	0.00073	0.00002	0.30028	0.00093	0.00021	0.00002	3.12087	0.10641	81.7	7.43	0.25

Table DR2

Laser Power (W)	^{40}Ar (moles)	^{40}Ar (mVolts)	± (mVolts)	^{39}Ar (mVolts)	± (mVolts)	^{38}Ar (mVolts)	± (mVolts)	^{37}Ar (mVolts)	± (mVolts)	^{36}Ar (mVolts)	± (mVolts)	$^{40}Ar^*/^{39}Ar$	±	$\%^{40}Ar^*$	Age (Ma)	± (Ma)
EEW02-20	J = 0.01203±0.00006															
step 1	4.259E-15	354.91	0.59	161.70	0.80	2.22	0.07	34.27	0.76	0.911	0.014	0.530	0.026	24.15	11.47	0.57
step 2	7.687E-15	640.59	1.44	416.15	0.45	5.06	0.07	108.04	0.42	2.051	0.014	0.083	0.011	5.37	1.79	0.23
step 3	6.271E-15	522.60	0.63	427.50	0.42	4.99	0.09	125.76	2.00	1.677	0.014	0.063	0.010	5.19	1.38	0.21
step 4	8.606E-15	717.18	1.06	709.93	0.60	9.15	0.09	224.23	0.56	2.141	0.032	0.119	0.013	11.79	2.58	0.29
Step 5	4.615E-15	384.61	0.76	446.58	0.76	5.46	0.09	132.11	1.44	1.095	0.014	0.137	0.010	15.86	2.96	0.21
Step 6	6.500E-15	541.68	1.32	649.80	1.33	8.38	0.16	207.67	0.90	1.465	0.022	0.167	0.010	20.07	3.63	0.23
Step 7	6.179E-15	514.88	0.73	592.35	2.86	7.61	0.22	191.47	0.86	1.409	0.014	0.166	0.007	19.11	3.60	0.16
Step 8	3.125E-15	260.44	0.63	350.55	1.67	4.27	0.07	136.93	2.98	0.694	0.022	0.158	0.019	21.27	3.43	0.41
Step 9	5.314E-15	442.87	0.90	566.24	2.05	6.91	0.08	286.14	6.59	1.204	0.022	0.154	0.012	19.63	3.33	0.26
Step 10	5.887E-15	490.59	2.05	676.37	2.51	8.15	0.16	462.14	3.86	1.288	0.014	0.163	0.007	22.42	3.53	0.15
Step 11	4.885E-14	4070.48	3.53	3894.26	10.24	51.77	1.90	3278.93	93.55	11.694	0.081	0.158	0.006	15.10	3.42	0.14
EEW02-2	J = 0.01203±0.00006															
step 1	3.350E-15	279.21	0.71	99.11	0.44	1.50	0.07	61.58	1.23	0.119	0.022	2.461	0.068	87.37	52.64	1.46
step 2	5.674E-16	47.29	0.56	14.17	0.28	0.21	0.05	3.12	0.36	0.009	0.010	3.146	0.221	94.27	67.01	4.64
step 3	2.159E-15	179.94	0.38	75.36	0.17	1.07	0.05	44.16	0.95	0.378	0.014	0.904	0.056	37.87	19.52	1.20
step 4	6.446E-16	53.72	0.37	43.11	0.17	0.34	0.05	9.42	0.85	0.022	0.014	1.097	0.097	88.04	23.65	2.09
step 5	1.069E-14	890.70	1.24	445.24	1.45	6.29	0.09	341.31	2.10	1.830	0.022	0.786	0.015	39.29	16.98	0.34
step 6	1.101E-14	917.91	1.17	474.82	1.21	5.73	0.10	463.82	14.64	1.908	0.014	0.746	0.009	38.59	16.12	0.22
step 7	7.149E-15	595.71	1.24	301.43	1.44	4.24	0.05	355.68	5.44	1.266	0.014	0.735	0.015	37.20	15.88	0.33
step 8	6.025E-15	502.05	1.47	268.85	0.27	3.23	0.06	417.77	5.75	1.040	0.014	0.725	0.016	38.80	15.66	0.36
step 9	1.163E-14	968.98	2.44	525.01	1.67	7.52	0.07	1190.61	27.86	1.986	0.010	0.728	0.008	39.44	15.73	0.18
step 10	2.186E-14	1821.70	2.98	1068.27	4.62	13.40	0.46	4690.86	255.92	3.842	0.040	0.643	0.012	37.68	13.89	0.26
EEWM2	J = 0.01203±0.00006															
step 1	2.358E-15	196.46	0.44	107.47	0.76	1.32	0.06	0.44	0.85	0.150	0.014	1.416	0.040	77.46	30.47	0.87
step 2	2.117E-16	17.64	0.36	0.21	0.15	0.04	0.05	-0.03	0.84	0.070	0.014	n.d.	n.d.	n.d.	n.d.	n.d.
step 3	n.d.	n.d.	n.d.	n.d.	n.d.	n.d.	n.d.	n.d.	n.d.	n.d.	n.d.	n.d.	n.d.	n.d.	n.d.	n.d.
step 4	1.339E-14	1115.63	1.65	794.81	6.77	8.46	0.19	1.07	0.86	0.450	0.014	1.236	0.012	88.09	26.64	0.29
step 5	1.340E-14	1117.07	1.78	841.88	5.19	9.27	0.30	3.24	0.85	0.249	0.014	1.239	0.009	93.41	26.70	0.24
step 6	1.732E-14	1443.47	2.95	1129.47	4.10	12.41	0.19	3.75	0.84	0.219	0.014	1.221	0.006	95.52	26.30	0.19
step 7	1.679E-14	1399.22	1.04	1028.14	6.12	12.06	0.30	3.99	0.85	0.449	0.014	1.232	0.008	90.52	26.54	0.22
step 8	1.973E-14	1643.82	2.15	1268.35	6.67	15.02	0.21	4.50	0.86	0.309	0.014	1.224	0.007	94.45	26.37	0.21
step 9	1.354E-14	1128.45	1.40	870.68	2.55	7.21	0.18	3.48	0.85	0.023	0.014	1.288	0.006	99.40	27.75	0.19
step 10	1.868E-14	1556.83	2.13	1235.77	4.19	10.42	0.25	5.06	0.86	0.239	0.014	1.203	0.006	95.47	25.92	0.18
EEW30	J = 0.01203±0.00006															
step 1	6.091E-15	507.59	0.47	87.71	0.25	1.39	0.06	0.48	0.30	1.380	0.014	1.138	0.048	19.67	24.54	1.04
step 2	9.532E-16	79.43	0.43	32.30	0.24	0.40	0.03	5.82	0.32	0.128	0.014	1.284	0.130	52.21	27.65	2.79
step 3	1.655E-15	137.93	0.40	47.13	0.20	0.53	0.04	5.19	0.44	0.199	0.014	1.681	0.089	57.45	36.13	1.91
step 4	1.239E-15	103.22	2.33	19.56	2.05	0.37	0.03	8.10	0.31	0.258	0.022	1.381	0.386	26.18	29.73	8.25
step 5	1.563E-15	130.26	0.39	81.02	0.39	0.79	0.04	6.91	0.33	0.068	0.014	1.359	0.052	84.53	29.26	1.12
step 6	7.643E-16	63.69	0.36	41.05	0.09	0.49	0.03	2.40	0.31	0.069	0.014	1.052	0.102	67.82	22.69	2.19
step 7	1.644E-15	137.04	0.39	70.53	0.36	0.96	0.03	3.16	0.33	0.179	0.010	1.192	0.043	61.37	25.69	0.92
step 8	2.980E-15	248.34	0.42	76.56	0.11	0.92	0.04	4.40	0.36	0.539	0.010	1.164	0.039	35.88	25.09	0.84
step 9	3.720E-14	3100.14	3.24	2279.92	2.82	23.41	0.11	84.85	0.44	1.198	0.020	1.205	0.003	88.58	25.95	0.15
step 10	4.700E-14	3917.06	3.40	2950.67	10.75	28.62	0.78	17.30	0.53	1.185	0.014	1.209	0.005	91.06	26.05	0.16
EEW02-5	J = 0.01203±0.00006															
step 1	3.866E-17	3.22	0.36	0.92	0.09	-0.05	0.03	-0.64	0.33	0.010	0.014	0.236	4.564	6.73	5.11	98.78
step 2	1.669E-16	13.91	0.36	0.26	0.09	-0.07	0.03	-0.36	0.31	0.030	0.014	19.475	17.523	36.06	379.74	308.12
step 3	4.296E-16	35.80	0.36	11.63	0.12	0.12	0.03	0.73	0.33	0.080	0.014	1.051	0.361	34.13	22.66	7.73
step 4	5.812E-15	484.30	0.55	324.42	1.33	3.85	0.08	11.23	0.44	0.277	0.014	1.240	0.014	83.10	26.72	0.33
step 5	1.280E-14	1066.75	1.97	812.69	2.83	8.49	0.18	19.91	0.78	0.455	0.010	1.147	0.006	87.40	24.73	0.18
step 6	7.830E-15	652.54	1.15	509.52	2.04	5.65	0.27	9.72	0.34	0.237	0.010	1.143	0.008	89.25	24.64	0.21
step 7	1.301E-14	1083.88	1.08	829.02	3.66	8.62	0.10	18.76	0.50	0.435	0.014	1.152	0.007	88.14	24.84	0.20
step 8	2.246E-14	1871.94	2.34	1412.79	4.37	16.60	0.27	26.57	0.53	0.773	0.022	1.163	0.006	87.80	25.07	0.18
step 9	1.837E-14	1531.24	2.77	1246.58	5.20	14.51	0.33	18.26	0.39	0.345	0.022	1.147	0.007	93.34	24.71	0.20
step 10	1.579E-14	1316.16	1.42	1082.91	2.84	12.15	0.04	17.10	0.32	0.335	0.014	1.124	0.005	92.47	24.23	0.16
step 11	1.505E-14	1254.47	1.74	893.45	4.62	9.96	0.21	16.14	0.34	0.756	0.014	1.154	0.008	82.20	24.88	0.21

<table>
<tr><th>Profile A – A'
(Dese – Bati
Accommodation
Zone
11°N to 11°15'N
and between
39°30'E and 40°E).</th><th>Composite of Profiles
B – B' and C – C'
(Kemise basin,
including, Borkena
draben, 10°15'N and
11°N.).</th><th>Profile D – D'
(Ataye basin)</th><th>Profile E – E'
(south Ataye
basin)</th><th>Profile F – F'
(Baso – Werena
basin)</th></tr>
<tr><td colspan="3">Dahla Series: at least 400 m fissural basalts ± discontinuous feldspar-rich fluvial sediments at base. Previously inferred to be older than the hominid-bearing 5.3 Ma Sagantole Formation (J. Quade, pers. comm., 2002).</td><td>Trachyte lavas
This sequence apparently offlaps units below and to the west.</td><td></td></tr>
<tr><td rowspan="5">Burka formation: unknown thickness intercalated basalts and rhyolites.

Dese basalt formation: at least 1000 m of heterogeneous basaltic to trachytic lavas measured adjacent to section A-A' (Fig. 6). Flows have smaller volumes and are more lithologically variable than the Oligocene flood basalts. Breccias and scoria cones mark discrete eruptive centers. Flows have variable thicknesses, and are internally unconformable within the formation. Flows around constructs dip more steeply than the flood basalts with the "excess" dip of the upper units caused by flow morphology and volcanic construction rather than rotation on fault blocks.</td><td rowspan="2">Bercha formation: at least 400 m of basaltic to intermediate centers; eroded basaltic cones and associated lava flows a few metres thick, scoriaceous basaltic flows and intermediate lava flows.</td><td rowspan="5">Senbete ignimbrite formation: at least ignimbrite-tuff pairs. from an unknown but more distal source than the centers feeding the Ataye or Kile rhyolite formations.
Mehal Wenz formation: 1-2 m-thick basaltic lavas and intercalated basaltic pyroclastics and ashes.
Kile rhyolite formation: vertical flow banded fabric defined by grey and black glassy bands.
Gadilo ignimbrite formation: distinctive near-source massive ignimbrites and rhyolitic ignimbrites.
Sar Amba formation: sequence of 1-2 m-thick basaltic lavas with scoriaceous flow tops and intercalated quartz-rich ash layers.
Ataye rhyolite formation: massive rhyolitic flows.</td><td colspan="2">Termaber Formation basaltic – trachytic shield volcanoe, e.g. Mezezo (Fig. 5).</td></tr>
<tr><td>Shewa Robit ignimbrite formation: Ignimbrites and tuffs with minor intercalated basaltic flows.

Insertu formation: rhyolitic centers, at least 400 m thick, intruded along fault planes.</td><td rowspan="3">Astit formation basaltic centers and contemporaneous dike-fed basaltic flows

Aliyu Amba ignimbrite formation: ignimbrite tuff pairs intruded by rhyolites.</td></tr>
<tr><td>Aneno formation: thickens rapidly eastwards to at least 200 m massive fissural basalts intruded by rhyolite domes. Flows extensive over 4 km but no visible intrusive centers, suggesting that the lavas were fed by dikes.</td><td>Birkitu formation: basaltic centers and associated lavas.</td></tr>
<tr><td>Kemise Rhyolite formation: at least 1500 m eroded (edges oversteepened) massive glassy and phenocryst-rich crystalline rhyolitic intrusions, glassy flow banded vertical intrusions, irregular to dome-shaped flows overlain and surrounded by block and ash units and rhyolitic ignimbrites. Vertically and laterally intrusive, and near-source extrusive, morphologies.</td><td>Rhyolitic centers: domes and associated breccias.</td></tr>
<tr><td colspan="5">Flood volcanic formations: voluminous, at least 2000 m thickness sections A-A' to D-D' and laterally homogeneous if not continuous for 10's of km, internally conformable basalt, trachyte lava flows, and with minor intercalated ignimbrites, air-fall tuffs and rhyolites. The flood volcanic group is 1000 m thick ~ 50 km west of profile E-E', where it overlies Archean-Proterozoic basement and Jurassic marine sediments (R. Pik, pers. comm., 2003).</td></tr>
</table>

Table DR 3. Summary of volcanostratigraphy this study. Informal formation names. New names this study in italics.

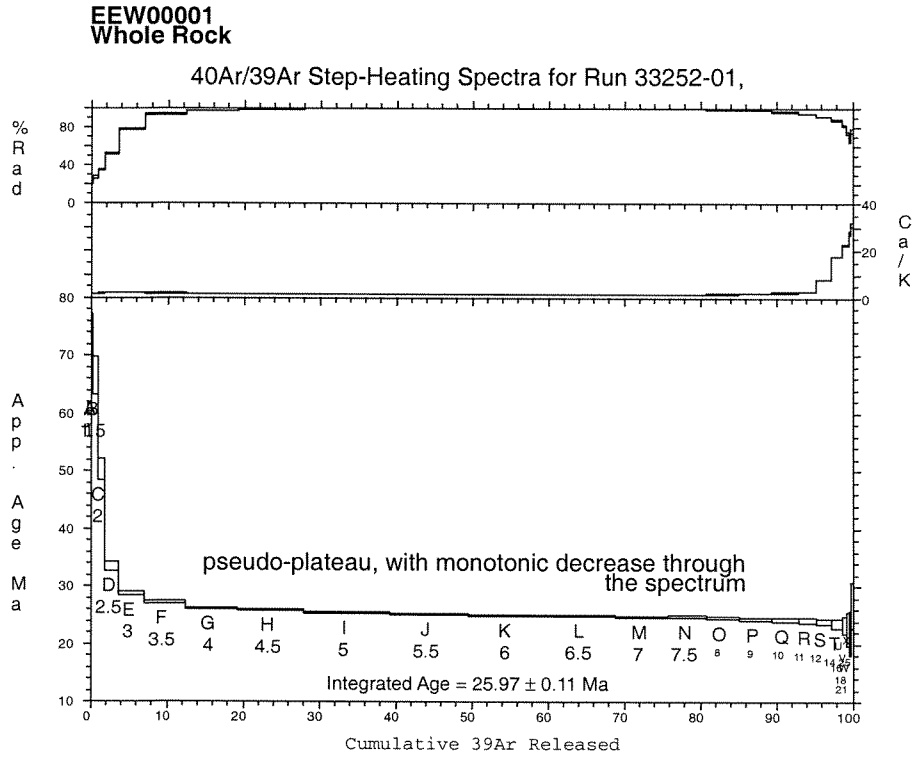

Figure DR2, Wolfenden et al.

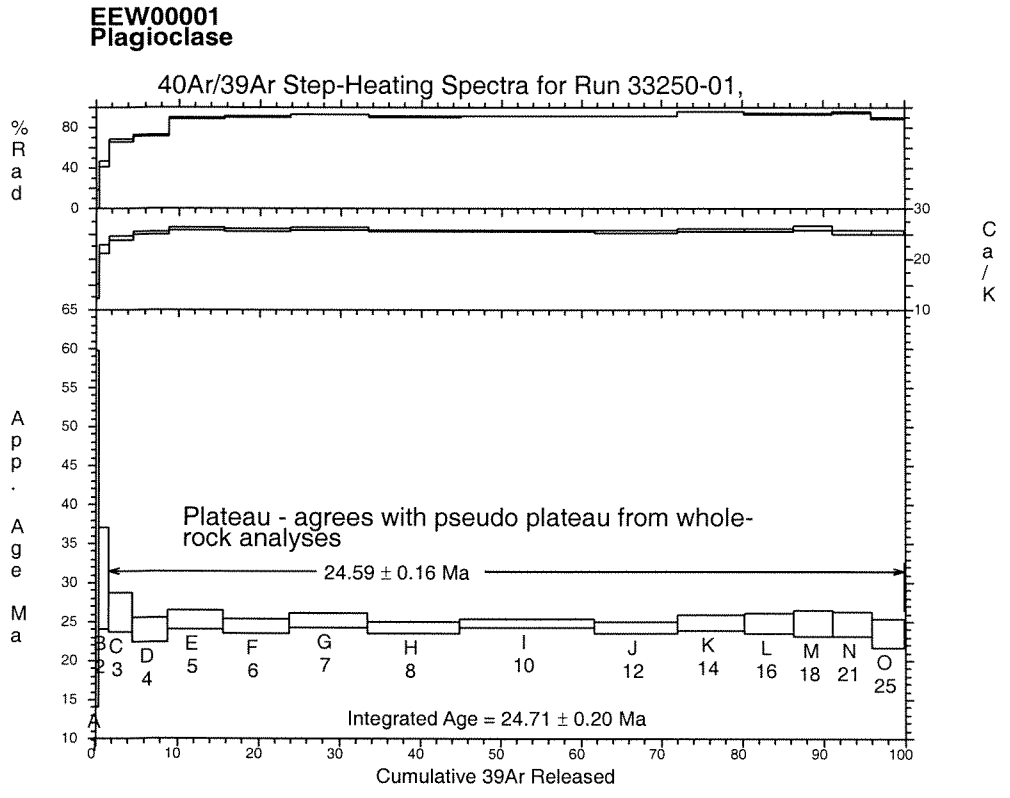

Figure DR3, Wolfenden et al.

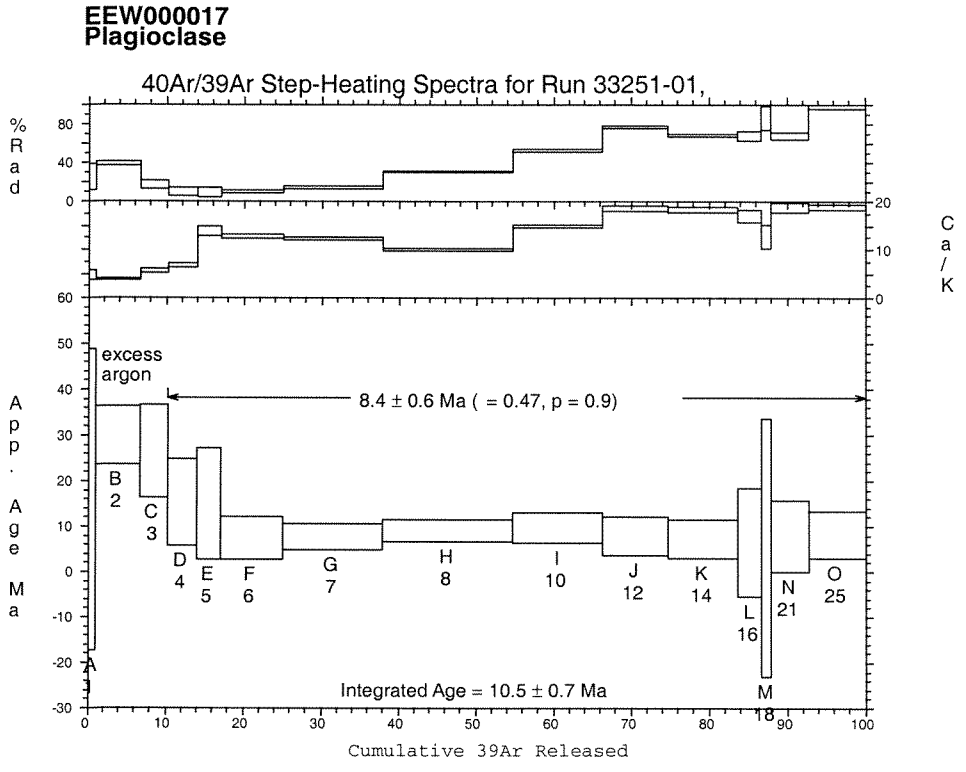

Figure DR4, Wolfenden et al.

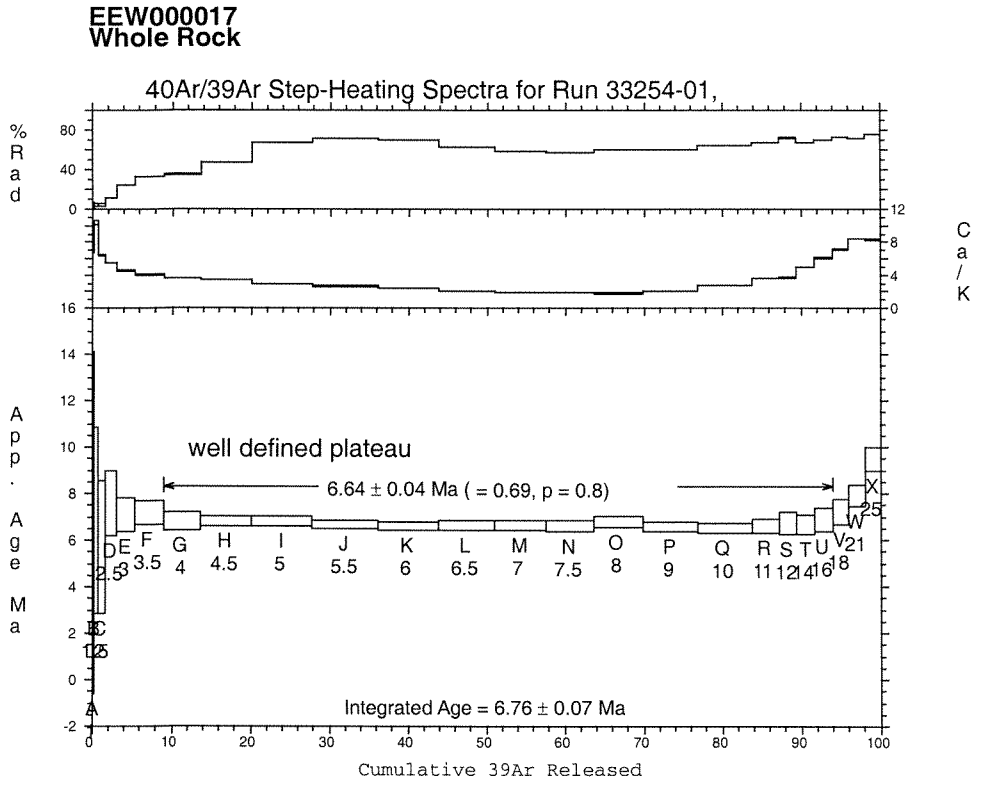

Figure DR5, Wolfenden et al.

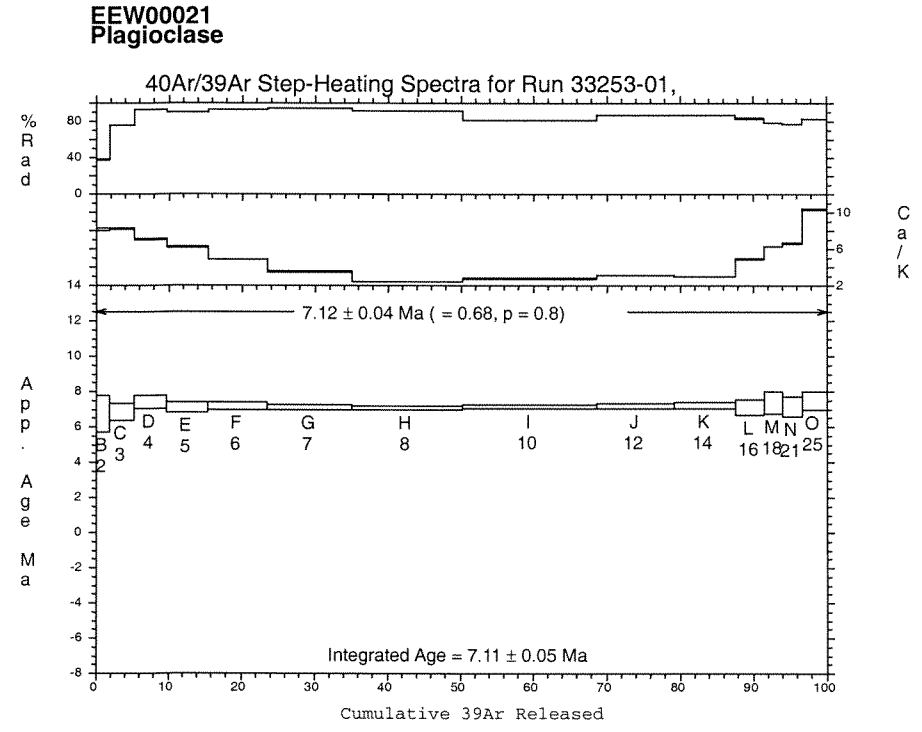

Figure DR6, Wolfenden et al.

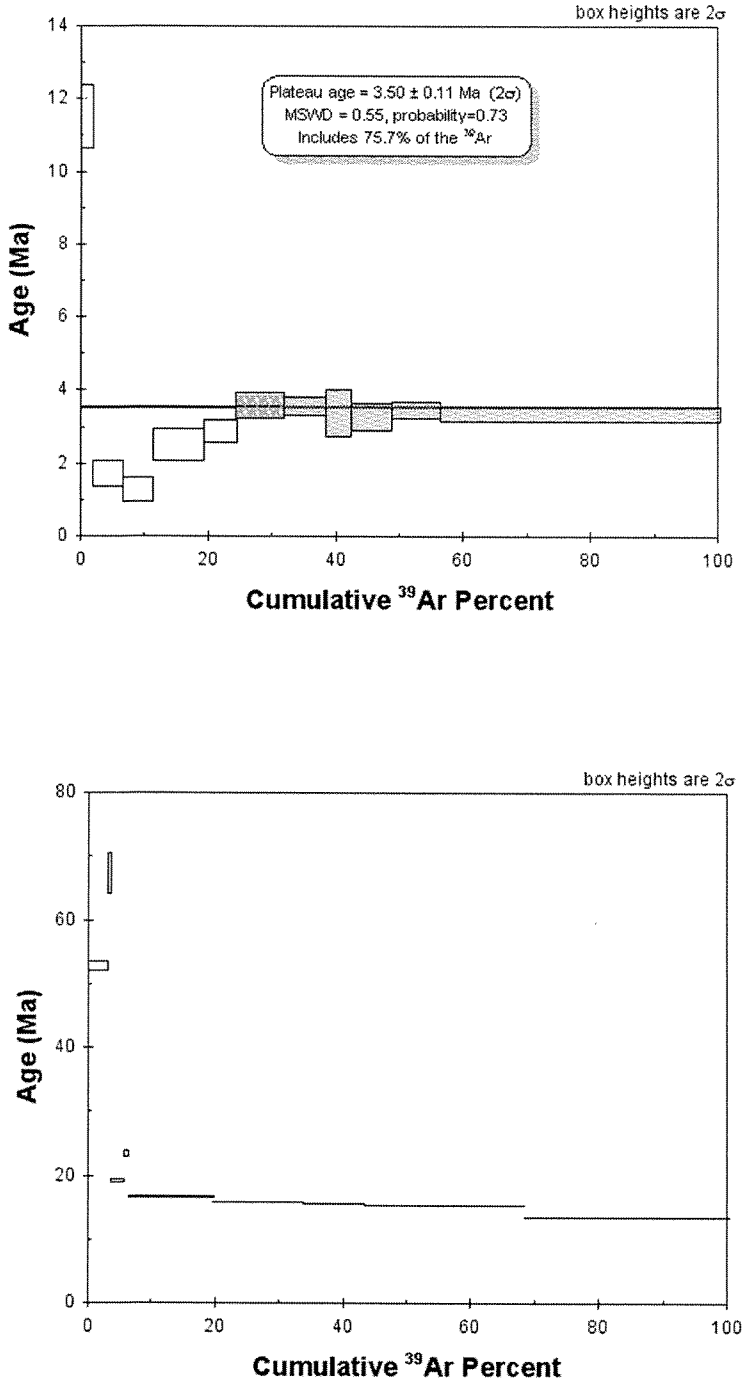

Figure DR7. a) EEW02-20 whole rock plateau ages. b) EEW02-2 whole rock plateau ages.

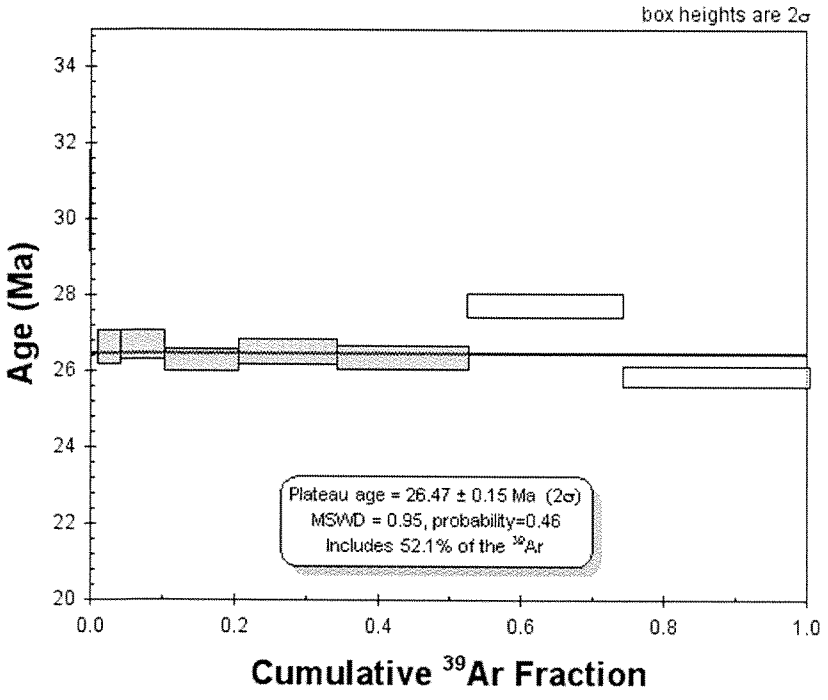

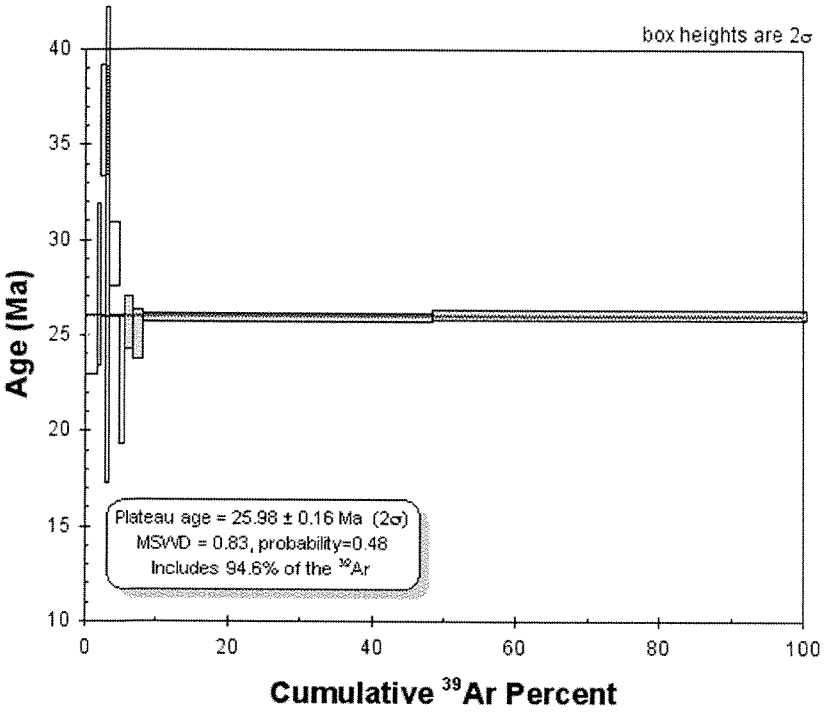

Figure DR8. a) EEWM2 whole rock plateau ages. b) EEW30 whole rock plateau ages.